Int J Adv Manuf Technol
DOI 10.1007/s00170-016-9407-5

ORIGINAL ARTICLE

freepaper.me FREE paper

Characteristics of welding and arc pressure in TIG narrow gap welding using novel magnetic arc oscillation

Jianfeng Wang[1,2] · Qingjie Sun[1,2] · Jicai Feng[1,2] · Shilu Wang[3] · Huanyao Zhao[2]

Received: 18 January 2016 / Accepted: 29 August 2016
© Springer-Verlag London 2016

Abstract Tungsten inert gas (TIG) narrow gap welding using magnetic arc oscillation is one of the most important methods for joining thick components. Today's developments are aimed at increasing a sophisticated process understanding, especially concerning the physical effect of arc behavior, which can provide many strategies to enhance weld prediction and joint quality. In this article, the arc behaviors studied by its arc pressure, static characteristic, and arc profile in terms of arc force are presented. With the help of the forces acting on the welding arc, arc profile can be considered separately to allow an improved investigation of narrow gap welding involved. Measurements of arc pressure distribution are used to validate the weld formation and the final welding result. Under the same conditions, the uniformity of arc pressure distribution in both the bottom and sidewall improved with the increase in magnetic flux density. Furthermore, a comparative study of arc static characteristic with magnetic field and non-magnetic field has also been carried out. The reduction in the difference of arc static characteristic is attributed to the inverse effect between electromagnetic pinch force and Lorentz force with the increasing welding current.

Keywords Magnetic arc · Narrow gap welding · Arc behavior · Arc pressure · Static characteristic

✉ Qingjie Sun
qjsun@hit.edu.cn

[1] State Key Laboratory of Advanced Welding and Joining, Harbin Institute of Technology, Harbin 150001, China

[2] Shandong Provincial Key Laboratory of Special Welding Technology, Harbin Institute of Technology at Weihai, Weihai 264209, China

[3] CIMC Raffles Offshore Engineering Co., Ltd., Yantai 264000, China

1 Introduction

The development of narrow gap welding has accelerated in recent years in the manufacture field of thick-walled components owing to a small heat affected zone resulting in minor distortions and significant cost savings [1–3]. Most of the processes are advanced with higher productivity in terms of robotization and automation [4]. Furthermore, the advent of magnetic arc welding offers great potentials of improving the sidewall penetration in the flat position [5–7], automatic joint tracking [8, 9], and preventing the molten pool sagging in the applications of horizontal and overhead welding [10, 11]. Therefore, the study on tungsten inert gas (TIG) narrow gap welding using novel magnetic arc oscillation is able to promote the development of heavy plate welding technology.

The main tasks of process development are to ensure a high process reliability and a high weld quality, but it is inevitably pointed out that the quality of arc welding greatly depends upon arc characteristics and behavior [12, 13]. It is known that arc plasma allows reliable information about arc characteristics and behavior [14]. The arc plasma carrying the arc current is a mixture of almost equal amounts of electrons and ions and required to ionize the gas in the arc column. The charged particles flow out from the electrode and are forwarded into the workpiece, which can be considered as a current conductor of gas that transforms electrical energy into heat energy [15]. Up to the present time, most investigators have concentrated on the understanding of arc plasma and their inherent properties to enhance weld prediction and joint quality [16–18]. The change in shape of the deflected arc is clearly visible [19]. However, given that the arc deflection is not always equal to the location of the largest energy input, then the shape of the deflected arc does not allow in accord with the distribution of heat input into the workpiece [20]. Also, arc pressure generated on the anode base metal is to understand physical arc

Published online: 02 September 2016

freepaper.me FREE paper

phenomena, which is an easier experimental method than former researchers have pursued [21, 22]. Increasing the arc pressure can cause a more concave surface of the weld pool [23]. In addition, the flow of the arc plasma may affect the molten pool. The distributions of temperature and velocity in molten pool can affect the weld geometry, microstructure, and mechanical properties [24]. Therefore, there is a significant interest in the representation of arc behavior.

To determine the effect of arc behavior on the flat workpiece, many factors should be considered routinely, such as heat flux, arc pressure, current density, arc shape, etc. The methods of the split anode and photography have been utilized. These methods allow the quantification of the arc behavior acting on the flat workpiece [20, 25]. However, in narrow gap welding, diagnostic to determine the exact arc behavior was rarely reported, specifically with additional magnetic field. Therefore, a basic understanding of the mechanisms of the magnetic arc physical effects involved in narrow groove is still imperative and will be the most useful for precise control of the weld geometry, process monitoring, and the arc stability. Notably, the emphasis is placed on the correlation between additional magnetic field and arc behavior including arc profile, arc force, arc pressure, and arc static characteristic.

2 Experimental procedure

The schematic of magnetic arc oscillation in the present study is shown in Fig. 1 [26]. The formation principle of magnetic arc oscillation is that a double field core acts as a magnetic conductor connecting to field coil. It is on both sides of the tungsten electrode and lowers into the narrow groove. As compared to the traditional type [5, 6], this new system is made smaller, lighter, and the magnetic flux density can increase. The arc is periodically oscillated by Lorentz interaction generated by the moving of welding current through the transversal alternating magnetic field.

The magnetic arc narrow gap welding head is shown in Fig. 2. The system consists of welding gun, electromagnet, and field core. The field core is built into the both sides of welding gun with an 8 mm thick. The field core is fed through the axial rectangular hole of the electromagnet. The magnetic field line is first generated by the electromagnet, and then the field core transmits the magnetic field line to the arc zone. Finally, the magnetic field is applied to the welding arc in parallel to the welding direction. The tungsten electrode is fed through the axial hole of the welding tip and the surface of the axial hole is coated with ceramic. Consequently, the body of the welding tip is insulated from the tungsten electrode. The welding tip made of red copper with high thermal conductivity is cooled by forced water flow to prevent its temperature from rising above its melting temperature. The length and width of the welding head are 280 and 150 mm, respectively. Furthermore, the length is mainly determined by the thickness of welding material.

A digital control power supply (Fronius, Magicwave 5000) is employed. The welding process is performed under the direct current electrode negative (DCEN) condition. During the experiments, the workpiece is fixed and the welding torch is moved at a constant speed of 60 mm/min. Pure argon at a constant rate of 25 L/min is supplied for shielding.

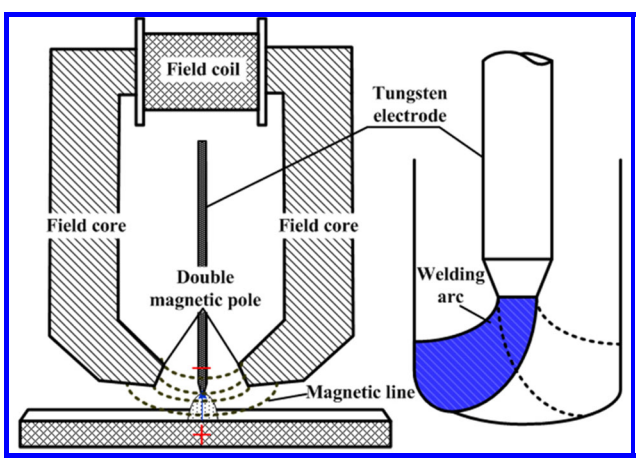

Fig. 1 Schematic of magnetic arc oscillation using double magnetic pole [26]

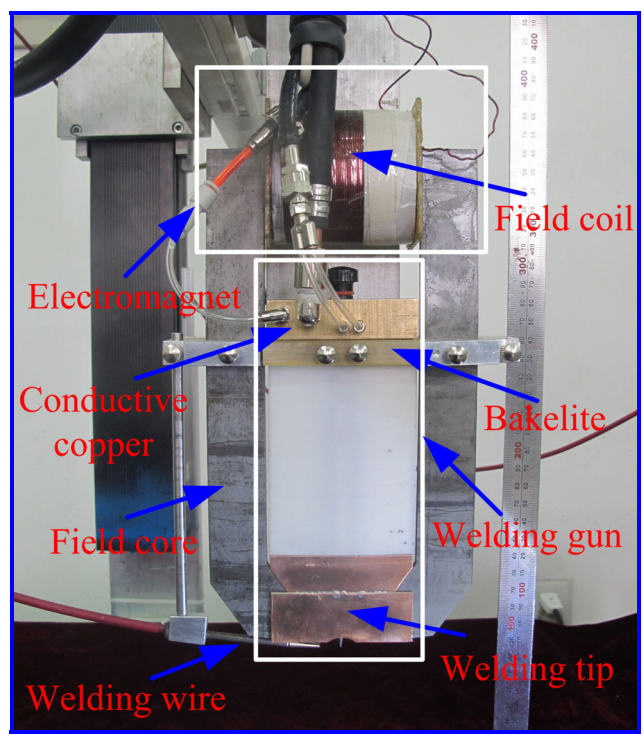

Fig. 2 Magnetic arc narrow gap welding head

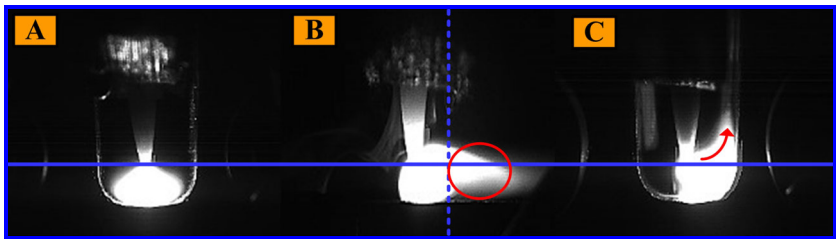

Fig. 3 Arc profile under different welding forms. **a** Non-magnetic field. **b** Magnetic arc welding without narrow groove. **c** Magnetic arc welding in narrow groove

3 Results and discussion

3.1 Arc profile

A notable characteristic of magnetic arc oscillation is the decentralized physical effects of the arc, which results in the expandation of the arc area acting on the workpiece and provides a shallow penetration. A high-speed video camera (1500 frames/s) is applied to capture arc profile under different welding forms in real time. The base plate with a gap geometry of 10-mm width is modified in a water-cooled red copper under the following conditions: a welding current of 200 A, contact tip-to-workpiece distance of 3 mm, magnetic field frequency of 10 Hz, and magnetic flux density of 6 mT.

Figure 3 illustrates arc profile under different welding forms. Due to optimum parameters, the welding arc is steady and seems to be bell-shaped during conventional TIG welding (non-magnetic field), as shown in Fig. 3a. When the magnetic field is applied to the welding arc, it is observed that whether or not the narrow gap welding head exists in narrow groove, the magnetic field plays a major role in the arc profile. When there is no narrow groove, the welding arc can be deflected perpendicular to the welding direction. Meanwhile, part of the arc is pushed away from the workpiece surface, as shown in Fig. 3b. With the existence of the narrow groove, the deflected arc is towards the corner between the sidewall and bottom. At the same time, the upward movement of the arc also appears in Fig. 3c. The reason of this behavior can be explained as follows.

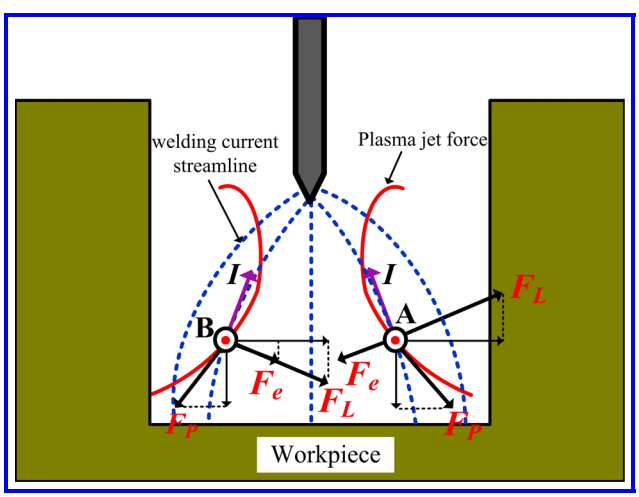

Fig. 4 Schematic of the forces acting on the arc with magnetic field

The forces affecting the arc determine the arc profile, as demonstrated by Qi et al. [18]. Therefore, it is necessary to analyze arc force condition in order to explore the influence mechanism of magnetic field on arc profile. It should be noted that plasma flow force and electromagnetic pinch force are recognized as the main compositions of arc force [27]. The electromagnetic pinch force can be expressed as

$$F_e = KI^2 ln(R_b/R_a) \tag{1}$$

where K is the electromagnetic coefficient, I is the welding current, R_b is the radius of arc undersurface, and R_a is the radius of arc top surface. The plasma flow force can be expressed as

$$\overline{F}_p = * \int_0^{\pi} \int_{-R_b}^{R_b} \frac{1}{2r} F_P \mathrm{d}r\mathrm{d}\theta = \frac{\pi \cdot a^2 F_{max}}{2R^2} \int_0^{R_b} \frac{r^3}{1-e^{-ar}(1+ar)} e^{-ar}\mathrm{d}r \tag{2}$$

where F_p is the average plasma flow force, F_P is the plasma flow force, F_{max} is the pressure at arc axes, r is the radial coordinate, and a is the distribution curve of concentration coefficient. Compared with the arc force condition in conventional TIG welding, the Lorentz force (F_L) will also affect the

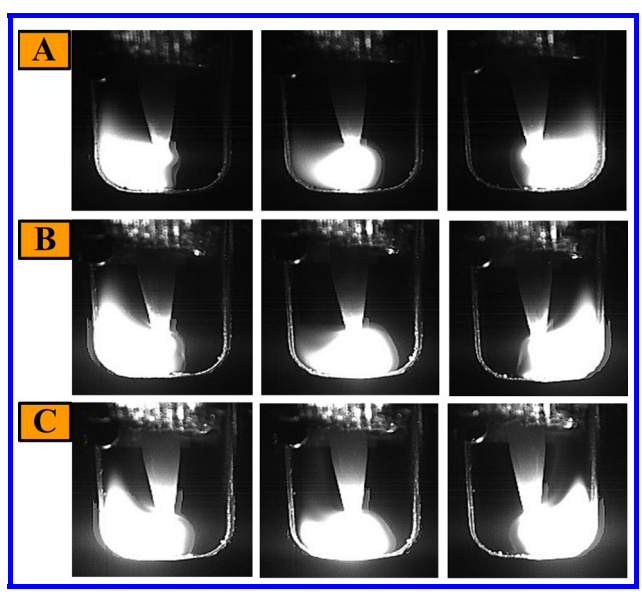

Fig. 5 Captured images of arc shape under different welding current. **a** 150 A. **b** 200 A. **c** 250 A

FREE paper freepaper.me دانلود کننده مقالات علمی

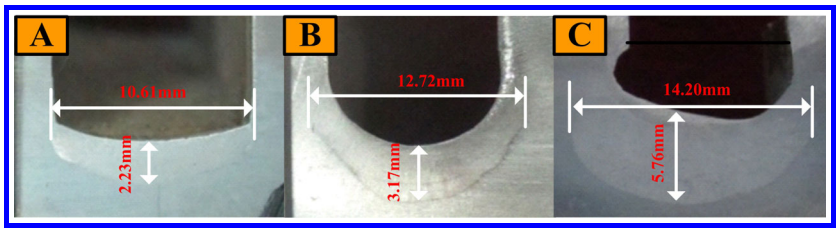

Fig. 6 Cross-sectional macrograph of joints under different welding current. **a** 150 A. **b** 200 A. **c** 250 A

arc owing to magnetic field externally applied to the welding arc. F_L is represented by

$$F_L = IBL \tag{3}$$

where B is the magnetic flux density, and L is the moving length of the particle per unit. The schematic of the force affecting the arc is shown in Fig. 4. Considering the difference of arc force in both sides of the arc axis, it is necessary to select two particles (locations A and B) as the research objects. The magnetic field direction is assumed to be perpendicular to the paper outward.

As seen in Fig. 4, the directions of plasma flow force and electromagnetic pinch force are based on the arc axis symmetry at the locations A and B. Furthermore, plasma flow force acts as the driving force of surface deformation in the molten pool. Electromagnetic pinch force plays an important role in arc stiffness. Therefore, the additional Lorentz force primarily affects the electromagnetic pinch force. The direction of Lorentz force is in the upper right at the location A and is in the bottom right at the location B. The difference of the Lorentz force between the both sides of arc axis can be considered as the nature of arc change. As the particles on the left side of arc axis move to workpiece along the bottom right and that on the right side of arc axis move far away from the workpiece along the upper right, the welding arc far from the arc axis is held up. When narrow groove is applied during TIG welding, the arc deflection is restrained along the welding width direction. Most of particles are clustered together in the corner between the sidewall and the bottom. In addition, part of particles has a potential of collision with that of workpiece, which changes the arc trajectory and presents the upward movement. This result suggests that the analysis of arc force is quite close to our experimental results in Fig. 3. It is concluded that the arc is deflected by the combination effect of these forces.

According to the analysis mentioned above, there is another interesting phenomenon that catches our attention. It is imperative to point out that electromagnetic pinch force and Lorentz force are both in proportion to the welding current, while the inverse effect between electromagnetic pinch force and Lorentz force causes the arc force analysis to be rather complex. According to Fig. 5, arc oscillation width is almost identical under different welding currents, i.e., the increasing current decreases the percentage of the welding arc acting on the sidewall. However, the sidewall and the weld penetrations are both apparently increased with the increase in welding current during the welding process, as shown in Fig. 6. Besides, the increment of weld penetration is higher than that of the sidewall penetration in some degree. Therefore, the variation of arc oscillation width cannot show a good agreement with that of the sidewall penetration.

In order to explain the difference between arc oscillation width and sidewall penetration, a split-anode method of Nestor [20, 25] is modified to a narrow gap geometry in order to allow the quantification of the welding current, given in Fig. 7. The welding current division ratio δ is characterized by the ratio of welding current flowing through the sidewall to

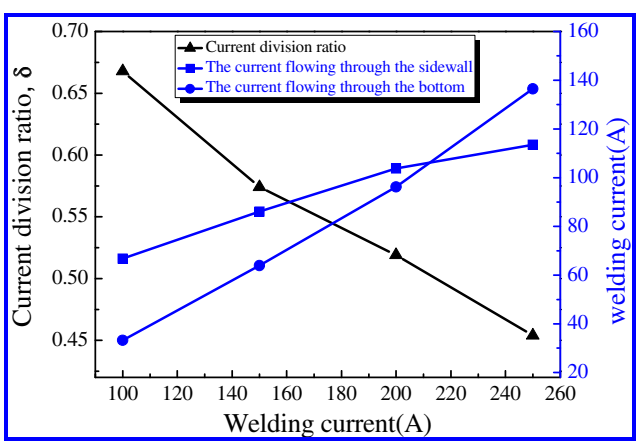

Fig. 7 Current division ratio and welding current flowing through the sidewall and bottom with different welding currents

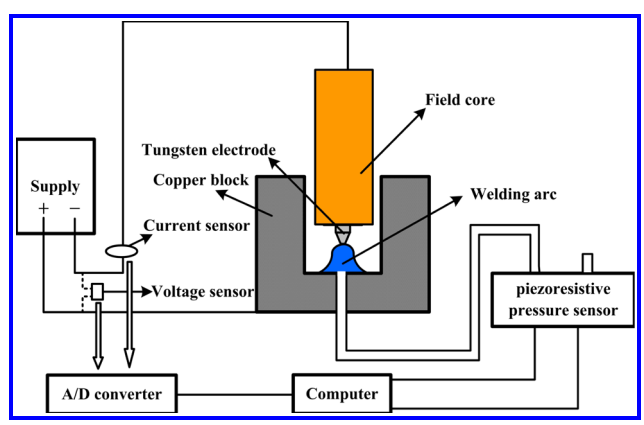

Fig. 8 Schematic diagram of the arc pressure measurement and the electrical acquisition system

FREE paper freepaper.me دانلود کننده مقالات علمی

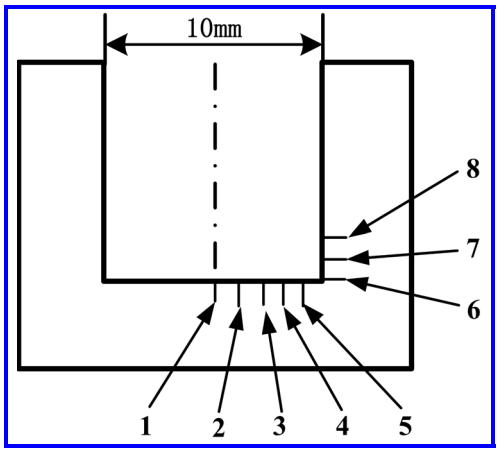

Fig. 9 Schematic of eight measuring points

the total welding current. With the increase in welding current, the fraction of the current flowing through the sidewall decreases, corresponding to the above analysis about the effect of welding current on arc oscillation width.

Figure 7 also illustrates that the value of the welding current flowing through the sidewall and bottom both increases rapidly with the increasing welding current. However, the increment of the sidewall is smaller than that of the bottom. Considering that welding current is directly proportional to the welding penetration [28], this implies that the results agree with the above results obtained in Fig. 6. Overall, in spite of the inverse effect between electromagnetic pinch force and Lorentz force, the analysis of arc force is suitable for magnetic arc behavior.

3.2 Arc pressure

The measurement of the arc pressure on the workpiece allows the characterization of the arc force on the molten pool surface and therefore the identification of physical arc phenomena, especially its effect on the penetration. A water-cooled copper plate with a gap geometry of 10-mm width and 10-mm depth is used to ensure steady boundary conditions, as shown in Fig. 8. A piezoresistive pressure sensor is utilized to detect the arc pressure in the bottom and sidewall of the narrow groove. Eight measuring bore holes with a diameter of 0.8 mm are installed at intervals of 1 mm along the narrow groove (Fig. 9), which are marked from 1 to 8.

Among the eight measuring points, the first and sixth measuring points are special because the first measuring point is at the center of the groove and the sixth measuring point is at the corner. The distribution of the arc pressure along the welding direction in the first measuring point under different magnetic flux densities is displayed in Fig. 10a. By extracting the maximum value of every distributed linetype, the histogram of the arc pressure in the first measuring point is shown in Fig. 10b. It can be seen that the maximum arc pressure without magnetic field is 197 Pa. Also, the maximum arc pressure decreases gradually with the increasing magnetic flux density. The maximum arc pressure reduces to 41 Pa as the density is 4 mT, about 20.8 % of that without magnetic field.

The distribution of the arc pressure along the welding direction in the sixth measuring point under different magnetic flux densities is shown in Fig. 11a. By extracting the maximum value of every distributed linetype, the histogram of arc pressure in the sixth measuring point is shown in Fig. 11b. The effect of magnetic flux density on maximum arc pressure is extremely important when applying the same welding parameters. The results indicate that the maximum arc pressure slightly increases with increasing magnetic flux density when the preset value is less than 3 mT. The maximum arc pressure reaches the peak value of 53 Pa at a magnetic flux density of 3 mT. When the magnetic flux density is greater than 3 mT, it can be inferred that due to the larger arc deflection, the arc impact force acting on the sixth measuring point decreases with the increasing of magnetic flux density, and thus decreases the maximum arc pressure.

The maximum arc pressure in the bottom and sidewall under different magnetic flux densities are illustrated in Fig. 12. The uniformity of arc pressure is obviously improved along weld width direction with the increasing magnetic flux

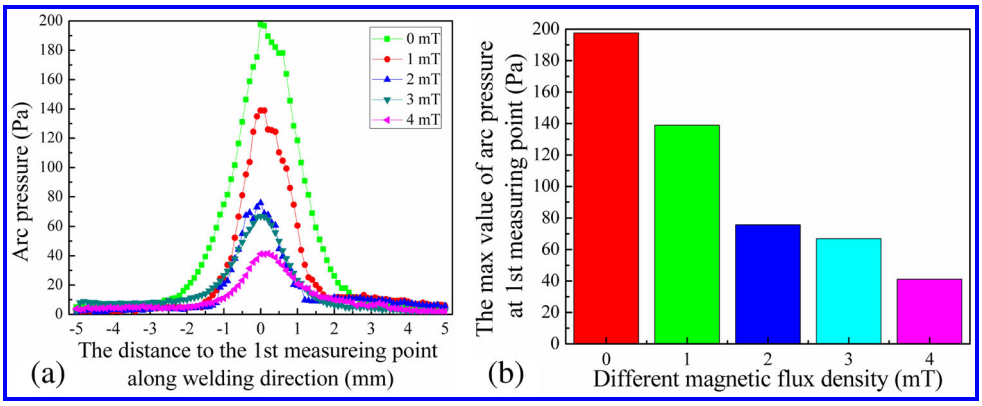

Fig. 10 Arc pressure in the first measuring point under different magnetic flux densities. **a** Arc pressure along the welding direction. **b** Max value of arc pressure

freepaper.me FREE paper

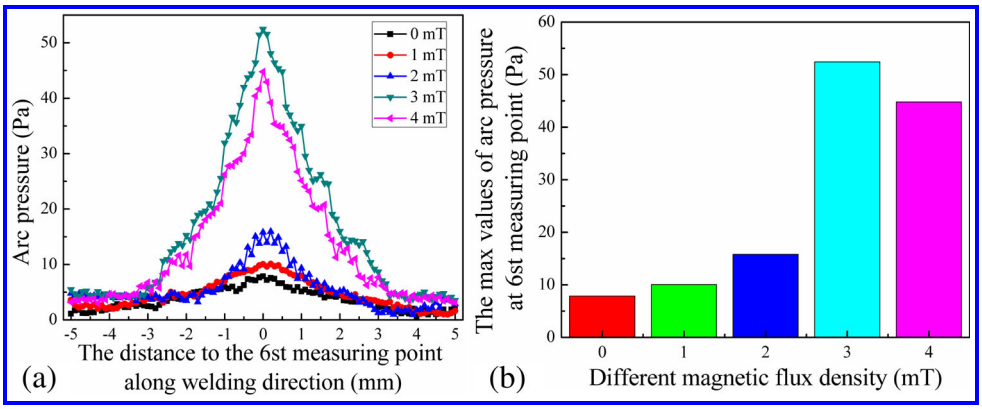

Fig. 11 Arc pressure in the sixth measuring point under different magnetic flux densities. **a** Arc pressure along the welding direction. **b** Max value of arc pressure

density. The increase in the arc pressure of the sidewall confirms the changes in arc deflection. These results are consistent with the principle of the magnetic arc method and help explain the phenomena in the effect of magnetic flux density on weld formation [26].

In Fig. 13, the maximum arc pressure of the bottom and sidewall under different welding currents is present. Arc pressure of all measuring points presents the even distribution for every welding current. Meanwhile, as the welding current increases, the arc pressure slightly increases from measuring point 1 to 7, which corresponds with the phenomena shown in Fig. 6. At the highest point 8, the arc pressure of 120 A is lower than that of 80 and 100 A. Such phenomenon can attribute to the degree of arc deflection which cannot be of unlimited increase at larger welding current for the same magnetic field parameters, due to the inverse effect between electromagnetic pinch force and Lorentz force. The results indicate that magnetic arc makes the distribution of arc pressure relatively more uniform.

3.3 Arc static characteristic

Magnetic arc oscillation leads to a change of arc length, which in turn periodically changes the arc voltage. Therefore, the additional magnetic field acting on welding arc changes the arc static characteristic. Hall effect sensor (LEM LT1005-S and LV 28-P) is employed to measure the welding current and voltage, as shown in Fig. 8.

Figure 14 shows the measured arc static characteristics with and without magnetic field. It can be observed that every curve displays three regions, i.e., drooping characteristic, flat characteristic, and rising characteristic. In addition, static characteristic curve of magnetic arc shows obvious upward trend owing to the larger arc length induced by arc deflection compared to conventional TIG welding. However, the increment in magnetic arc voltage is lower than that of non-magnetic arc with the increasing welding current. In other words, the change in the static characteristic of conventional welding arc is more pronounced than that of magnetic arc with the increasing welding current. The reason for this phenomenon

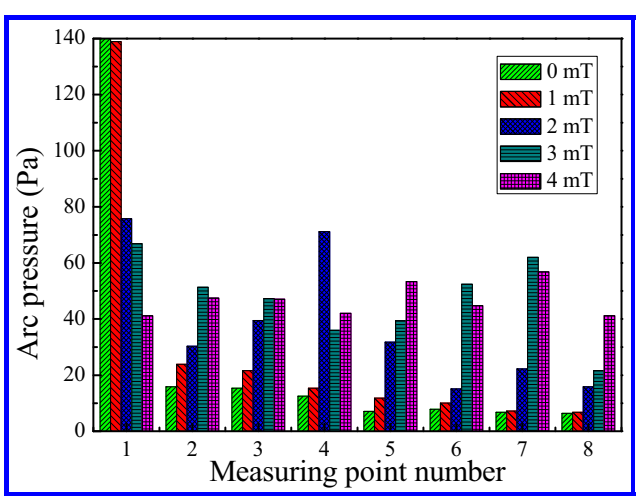

Fig. 12 The maximum arc pressure of eight measuring points in the bottom and sidewall under different magnetic flux densities

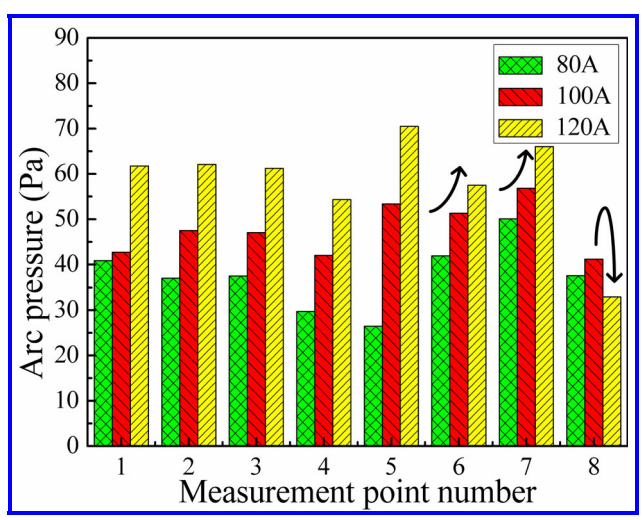

Fig. 13 The maximum arc pressure of eight measuring points in the bottom and sidewall under different welding currents

freepaper.me FREE paper

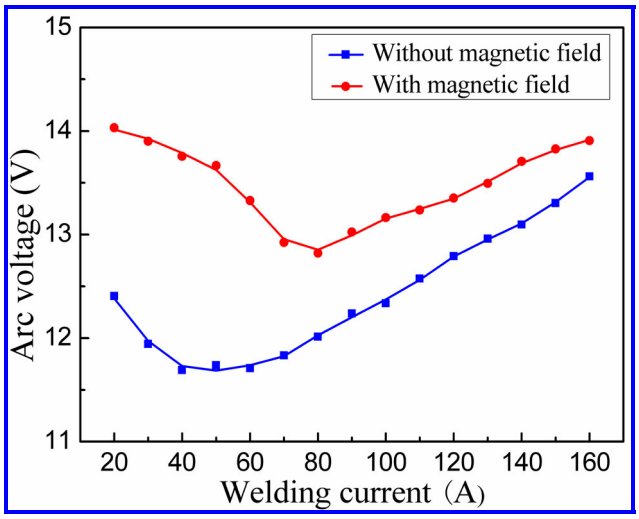

Fig. 14 Static characteristic curve of the welding arc with and without magnetic field

is due to the inverse effect between electromagnetic pinch force and Lorentz force. According to Eqs. 1 and 3, electromagnetic pinch force and Lorentz force are both in proportion to the welding current. The former is a retaining force that can restrict the arc deflection, while the latter is a detaching force that can promote the arc deflection. As the welding current increases, these two forces both increases, which means that the inverse effect between the two forces is more obvious. In this situation, the degree of inverse effect between the two forces (λ) is characterized by the ratio of electromagnetic pinch force to Lorentz force qualitatively:

$$\lambda = \frac{F_e}{F_L} = I \cdot \frac{K\ln(R_b/R_a)}{BL} \tag{4}$$

Based on Eq. 4, the value of λ is directly proportional to the value of I. At low welding current, the λ value is too small and the Lorentz force (F_L) is dominated, leading to the larger arc oscillation width. Hence, the arc voltage of magnetic arc is substantially higher compared to non-magnetic arc when the welding current is lower. As the welding current increases, the λ value increases and the Lorentz force (F_L) is subordinate, while the electromagnetic pinch force (F_e) is dominated. In this case, due to the larger retaining force, the magnetic arc cannot be sufficiently deflected for the same magnetic field parameters. So the difference of arc static characteristic with magnetic field and non-magnetic field decreases gradually with increasing welding current. This finding suggests that the arc oscillation width is seriously affected by the welding current. If the welding current is higher enough, the welding current has maximal effect on the variation of arc oscillation width. It is concluded that arc deflection induced by the magnetic field changes the static characteristic of the welding arc compared with conventional TIG welding.

4 Conclusions

From the present study, arc behavior of magnetic arc has been explored. Arc profile, static characteristic, and arc pressure should be considered when ascertaining the physical effect of arc behavior. Some conclusions can be obtained that:

1. Under the action of magnetic field, the magnetic arc is deflected and presents a trend of the upward movement, which is caused by additional Lorentz force and sidewall restraint.
2. Arc pressure of the bottom decreases while that of the sidewall increases as magnetic flux density increases. Magnetic arc renders the distribution of arc pressure relatively more uniform.
3. There are three static characteristic regions referring to drooping characteristic, flat characteristic, and rising characteristic for TIG welding with and without magnetic field. The voltage of magnetic arc is invariably higher than that of non-magnetic arc, and the difference decreases with the increasing welding current.

Acknowledgments We are grateful to the National Natural Science Foundation of China (Grant No. 51475104, 51435004) and the State Key Development Program for Basic Research of China (Grant No. 2013CB035500) for the financial support to this study.

References

1. Li WH, Gao K, Wu J, Hu T, Wang JY (2014) SVM-based information fusion for weld deviation extraction and weld groove state identification in rotating arc narrow gap MAG welding. Int J Adv Manuf Technol 74(9–12):1355–1364
2. Cui HC, Jiang ZD, Tang XH, Lu FG (2014) Research on narrow-gap GMAW with swing arc system in horizontal position. Int J Adv Manuf Technol 74(1–4):297–305
3. Xu WH, Lin SB, Fan CL, Yang CL (2014) Evaluation on microstructure and mechanical properties of high-strength low-alloy steel joints with oscillating arc narrow gap GMA welding. Int J Adv Manuf Technol 75(9–12):1439–1446
4. Nomura EK, Morisaki MK, Hirata EY (2009) Magnetic control of arc plasma and its modelling. Weld World 53(7–8):R181–R187
5. Sun QJ, Hun HF, Li WJ, Liang YC (2013) Electrode tips geometry and penetrating in narrow gap welding. Sci Technol Weld Join 18(3):198–203
6. Belous VY (2011) Conditions for formation of defect-free welds in narrow-gap magnetically controlled arc welding of low titanium alloys. Paton Weld J 3:16–18
7. Belous VY, Akhonin SV (2007) Influence of controlling magnetic field parameters on weld formation in narrow-gap argon-arc welding of titanium alloys. Paton Weld J 59(4):2–5
8. Kang YH, Na SJ (2003) Characteristics of welding and arc signal in narrow groove gas metal arc welding using electromagnetic arc oscillation. Weld J 82(5):93–99
9. Belous VY, Akhonin SV (2011) System for automatic regulation of position of tungsten electrode in narrow-gap magnetically controlled arc welding of titanium. Paton Weld J 7:30–33

دانلود کننده مقالات علمی freepaper.me FREE paper

10. Shoichi M, Yukio M, Koki T, Yasushi T, Yukinori M, Yusuke M (2013) Study on the application for electromagnetic controlled molten pool welding process in overhead and flat position welding. Sci Technol Weld Join 18(1):38–44
11. Yukio M, Satoru Z, Yoshinori H (2000) Method of welding in the horizontal position and welding apparatus. United States patent: 6023043
12. Ghosh PK, Gupta SR, Randeiwa HS (1999) Characteristics and criticality of bead on plate deposition in pulsed current vertical-up GMAW steel. Int J Join Mater 11(4):99–111
13. Ghosh PK, Dorn L, Kulkarni S, Hofmann F (2009) Arc characteristics and behaviour of metal transfer in pulsed current GMA welding of stainless steel. J Mater Process Tech 209(3):1262–1274
14. Kah P, Latifi H, Suoranta R, Martikainen J, Pirinen M (2014) Usability of arc types in industrial welding. Int J Mech Mater Eng 9(1):1–12
15. Lancaster JF (1984) The physics of welding. Phys Tech 15(2):73–79
16. Xu G, Hu J, Tsai HL (2009) Three-dimensional modeling of arc plasma and metal transfer in gas metal arc welding. Int J Heat Mass Tran 52(7):1709–1724
17. Howse DS, Lucas W (2000) Investigation into arc constriction by active fluxes for tungsten inert gas welding. Sci Technol Weld Join 5(3):189–193
18. Qi BJ, Yang MX, Cong BQ, Liu FJ (2013) The effect of arc behavior on weld geometry by high-frequency pulse GTAW process with 0Cr18Ni9Ti stainless steel. Int J Adv Manuf Technol 66(9–12): 1545–1553
19. Li W, Gao K, Wu J, Wang JY, Ji YH (2014) Groove sidewall penetration modeling for rotating arc narrow gap MAG welding. Int J Adv Manuf Technol 78(1–4):573–581
20. Häßler M, Rose S, Füssel U, Schneider HI, Werner C (2015) TIG narrow gap welding—new approaches to evaluate and improve the shielding gas coverage and the energy input. Weld World 59(1):71–76
21. Oh DS, Kim YS, Cho SM (2005) Derivation of current density distribution by arc pressure measurement in GTA welding. Sci Technol Weld Join 10(4):442–446
22. Li TQ, Wu CS (2015) Numerical simulation of plasma arc welding with keyhole-dependent heat source and arc pressure distribution. Int J Adv Manuf Technol 78(1–4):593–602
23. Murphy AB, Tanaka M, Yamamoto K, Tashiro S, Lowke JJ (2009) CFD modelling of arc welding: the importance of the arc plasma. In Seventh International Conference on CFD in the Minerals and Process Industries, Melbourne, Australia, p 1–6
24. Fan HG, Kovacevic R (2004) A unified model of transport phenomena in gas metal arc welding including electrode, arc plasma and molten pool. J Phys D Appl Phys 37(18):2531–2544
25. Nestor OH (1962) Heat intensity and current density distributions at the anode of high current, inert gas arcs. J Appl Phys 33(5):1638–1648
26. Sun QJ, Wang JF, Cai CW, Li Q, Feng JC (2015) Optimization of magnetic arc oscillation system by using double magnetic pole to TIG narrow gap welding. Int J Adv Manuf Technol. doi:10.1007/s00170-015-8214-8
27. Ando K, Hasegawa M (1985) Welding arc phenomena [M]. Beijing China Mach 249–250 (in Chinese)
28. Kim IS, Son JS, Kim IG, Kimc JY, Kimd OS (2003) A study on relationship between process variables and bead penetration for robotic CO_2 arc welding. J Mater Process Tech 136(1):139–145

دانلود کننده مقالات علمی freepaper.me FREE paper